# Effects of Baffle on Separated Convection Step Flow of Radiating Gas in a Duct

**M. Atashafrooz***
Department of Mechanical Engineering,
Sirjan University of Technology, Sirjan, Iran
E-mail:Meysam.atashafrooz@yahoo.com
*Corresponding author

**S. A. Gandjalikhan Nassab**
Department of Mechanical Engineering,
Shahid Bahonar University of Kerman, Iran
E-mail: ganj110@uk.ac.ir

**E. Sadat Behineh**
Department of Chemical Engineering,
Shiraz University of Technology, Iran
E-mail: elham_sbehineh@yahoo.com

**Received: 22 January 2015, Revised: 30 April 2015, Accepted: 28 June 2015**

**Abstract:** In this paper, the effects of baffle on thermal characteristics of combined convection-radiation heat transfer in laminar flow adjacent to an inclined backward facing step (BFS) in a horizontal duct are investigated. A baffle is mounted on the top wall of channel downstream side of step. In this study, the fluid is treated as a gray, absorbing, emitting and scattering medium; therefore, in the energy equation besides the convective and conductive terms, radiation term is also presented. The radiative transfer equation (RTE) is solved numerically by the discrete ordinates method (DOM) to find the divergence of radiative heat flux distribution inside the radiating medium. The blocked off method is employed for both fluid mechanic and radiation problems to simulate the presence of both step and baffle. The effects of height, width and location of baffle in channel and also the effects of radiative parameters on the fluid flow and heat transfer are investigated by plotting the variations of streamlines, Nusselt number and mean bulk temperature along the flow. It is revealed that, baffle and radiative parameters have great influences on flow and the thermal behaviors of systems with combined convection-radiation heat transfer.

**Keywords:** Baffle, Backward facing step, Blocked-off method, Convection-radiation heat transfer, DOM

**Reference:** Atashafrooz, M., and Gandjalikhan Nassab, S. A., "Effects of baffle on separated convection step flow of radiating gas in a duc**t**", Int J of Advanced Design and Manufacturing Technology, Vol. 8/ No. 3, 2015, pp. 33-47.

**Biographical notes: M. Atashafrooz** is an assistant professor in mechanical engineering in the Sirjan University of Technology, Sirjan, Iran. He received his MSc and PhD degrees from Shahid Bahonar University of Kerman in 2011 and 2015, respectively. He has several published papers about radiation heat transfer. **S. A. Gandjalikhan Nassab** is a professor in mechanical engineering in the Faculty of Engineering, Shahid Bahonar University, Kerman, Iran. He received his PhD from Shiraz University, Shiraz, Iran in 1999. He has several published papers about radiation heat transfer and in the CFD research area. **E. Sadat Behineh** received her MSc from Shiraz University of Technology in 2014. Her areas of interests are heat transfer in ducts and biodiesel.

## 1 INTRODUCTION

Separation flow and subsequent reattachment appear in many industrial applications due to a sudden expansion or contraction in the flow passages, such as backward and forward-facing steps, respectively. Separating and reattaching regions perform an important influence in the design of a wide variety of technological and engineering applications where heating or cooling process is required. Such flows accompanied with heat transfer are frequently encountered in many systems, such as power generating equipments, cooling of electronic systems, heat exchangers, gas turbine blades, combustion chamber and ducts flows used in industrial applications. Radiative heat transfer plays an important role in heat transfer in some of the mentioned devices, specially, when soot particles exist in the combustion product, the radiation effect may be important.

Besides, the trend toward increasing temperature in modern technological systems has promoted concerted effort to develop more comprehensive and accurate theoretical methods to treat radiation. Therefore, for having more accurate and reliable results in the analysis of these types of flow, the flowing fluid must be considered as a radiating medium and all of the heat transfer mechanisms including convection, conduction and radiation, must be taken into account. Backward facing step (BFS) or forward facing step (FFS) is one of the most fundamental geometries where the flow over them has the most features of separated flows. Although the geometry of BFS or FFS flow is very simple, the heat transfer and fluid flow over these types of step contain most of complexities. Consequently, it has been used in the benchmark investigations. There are many studies about separated-reattached convection flow over BFS in a duct by several investigators [1- 5].

Erturk [6] investigated the characteristics of flow over a two dimensional BFS in a wide range of Reynolds numbers. The two-dimensional Navier–Stokes equations for incompressible steady flows were solved with a very efficient finite difference numerical method which proved to be highly stable even at very high Reynolds numbers. Abu-Nada [7-9] analyzed the convection flow over a backward facing step in a duct to investigate the amount of entropy generation in this type of flow. A review of research on laminar convection flow over backward and forward facing steps was done by Abu-Mulaweh [10].

The purpose of this work was to give a detailed summery of the effect of several parameters such as step height, Reynolds number, Prandtl number and the buoyancy force on the flow and temperature distributions downstream of the step. There are many engineering applications, in which the forward or backward-facing step is inclined. Simulations of three-dimensional laminar forced convection adjacent to inclined backward-facing step in rectangular duct were presented by Chen et al., [11] to examine the effects of step inclination on flow and heat transfer distributions. Velocity, temperature, Nusselt number and friction coefficient distributions were presented in that study. The effects of step inclination angle on Nusselt number and friction coefficient distributions were shown by plotting many figures. Investigation of entropy generation in laminar forced convection gas flow over a recess including two inclined backward and forward facing steps in a horizontal duct was studied by Atashafrooz et al., [12-13]. The computational fluid dynamic (CFD) techniques were used to solve the governing equations. The effects of bleeding coefficient and recess length on the flow and heat transfer behaviors of the system were investigated in this work.

Although there are many research works about separation flows over FFS or BFS, but the fluid flow with heat transfer over these geometries considering baffle received less attention. In a recent study, Bahrami et al., [14] analyzed the effects of baffle on entropy generation in separated convection flow adjacent to inclined backward-facing step. In that work, numerical expressions, in terms of Nusselt number, entropy generation number, Bejan number (Be) and coefficient of friction were derived in dimensionless form. Numerical simulations of three-dimensional laminar forced convection flow adjacent to backward-facing step in a rectangular duct were used to examine effects of a baffle on the flow and heat transfer by Nie et al. [15]. In another research, analysis of turbulent flow and heat transfer over a double forward facing step with obstacles was studied by Oztop et al., [16].

In all of the mentioned studies, the effect of radiative heat transfer in fluid flow was neglected, such that the gas energy equation only contains the convection and conduction terms. In a forced convection problem, when the flowing gas behaves as a participating medium, its complex absorption, emission and scattering introduce a considerable difficulty in the simulation of these flows. There are limited numbers of literatures about the radiative transfer problems in convection flows with complex 2-D and 3-D geometries.

Bouali and Mezrhab [17] studied heat transfer by laminar forced convection with considering surface radiation in a divided vertical channel with isotherm side walls. They found that the surface radiation has important effect on the Nusselt number in convective flow with high Reynolds numbers.

The study of mixed convection heat transfer in 3-D horizontal and inclined ducts with considering gas radiation effects has been numerically examined in detail by Chiu et al., [18-19]. Those works were primarily focused on the interaction of the thermal radiation with mixed convection for a gray fluid in rectangular ducts. The vorticity–velocity method was employed to solve the three-dimensional Navier–Stokes equations while the integro-differential radiative transfer equation was solved by the discrete ordinates method. Results revealed that radiation effects have a considerable impact on the heat transfer and would reduce the thermal buoyancy effects. Besides, it was revealed that the development of temperature was accelerated by the radiation effects.

Three-dimensional combined convective-radiative heat transfer over a horizontal backward-facing step was studied by Ko and Anand [20] and Atashafrooz and Gandjalikhan Nassab [21]. In addition, the present authors [22-23] studied numerical analysis of combined convection-radiation heat transfer over a recess including two inclined backward and forward facing steps in a horizontal duct. The fluid is treated as a gray, absorbing, emitting and scattering medium. The role of radiation heat transfer on convection flow of a radiating gas was studied in detail. Also, there are several similar studies on this subject with different flow geometries by several other investigators [24-29].

Although there are some studies about combined convection and radiation heat transfer over a BFS and FFS, but based on the author's knowledge, laminar forced convection flow of radiating gas over an inclined backward facing step considering baffle, is still not studied theoretically or experimentally. Since, this flow geometry has many engineering applications; therefore, the main objective of present research work is to examine the heat transfer enhancement of laminar forced convection flow of a radiating gas adjacent to inclined backward-facing step by using a baffle installation onto the channel wall, while the well known block-off method and DOM are employed to solve the fluid mechanic and radiation problems.

## 2 PROBLEM DESCRIPTION

Laminar flow and combined convection and radiation heat transfer in a channel over an inclined backward facing step are numerically simulated to examine effects of the baffle on flow and heat transfer distributions. Geometry of the problem is shown in Fig. 1. The backward facing step is considered to be inclined with inclination angle of $\phi = 45^\circ$, which is evaluated from the horizontal sense. The upstream and downstream heights of the duct are h and H, respectively, such that this geometry provides the step height of s, with expansion (ER=H/h) ratio of 2. The upstream length of the duct is considered to be $L_1$=3H and the rest of the channel length is equal to $L_2$=25H. This is made to ensure that the flows at the inlet and outlet sections are not affected significantly by the sudden changes in the geometry and flow at the exit section becomes fully developed.

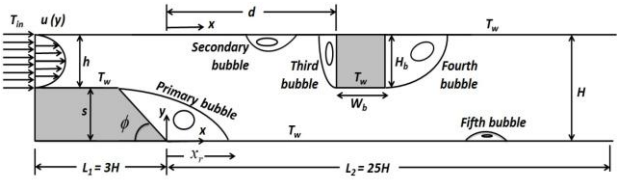


**Fig. 1** Schematic of computational domain

For the purpose of controlling the flow and heat transfer behaviors of the convection-radiation system, a baffle is mounted onto the top wall and after inclined BFS. The distance of the baffle from the inclined backward-facing step depicted by d is considered in a broad range from 1.5H to 12.5H in different test cases. The height and width of baffle are varied and are considered by $H_b$ and $W_b$, respectively.

## 3 BASIC EQUATIONS

The fundamental governing equations for present study are the conservations of mass, momentum and energy. For two-dimensional laminar flow, incompressible, steady and in the Cartesian coordinate system, these equations can be written as follows:

Conservation of mass:

$$\frac{\partial u}{\partial x}+\frac{\partial v}{\partial y}=0 \tag{1}$$

Conservation of momentum:

$$u\frac{\partial u}{\partial x}+v\frac{\partial u}{\partial y}=-\frac{1}{\rho}\frac{\partial p}{\partial x}+\frac{\mu}{\rho}\left(\frac{\partial^2 u}{\partial x^2}+\frac{\partial^2 u}{\partial y^2}\right) \tag{2}$$

$$u\frac{\partial v}{\partial x}+v\frac{\partial v}{\partial y}=-\frac{1}{\rho}\frac{\partial p}{\partial y}+\frac{\mu}{\rho}\left(\frac{\partial^2 v}{\partial x^2}+\frac{\partial^2 v}{\partial y^2}\right) \tag{3}$$

Conservation of energy:

$$\frac{\partial}{\partial x}(\rho u c_p T)+\frac{\partial}{\partial y}(\rho v c_p T)=\kappa\left(\frac{\partial^2 T}{\partial x^2}+\frac{\partial^2 T}{\partial y^2}\right)-\nabla.\vec{q}_r \tag{4}$$

In these equations, u and v are the velocity components in x- and y- directions, respectively, T the temperature, $\mu$ the dynamic viscosity, $\rho$ the density, p the

pressure, $c_p$ the specific heat, $\kappa$ the thermal conductivity and $\vec{q}_r$ is the radiative flux vector.

### 3.1. Gas Radiation Modeling

Since the gas is considered as a radiating medium, all of the convection, conduction and radiation terms are presented in the energy equation. Thus, to obtain the temperature distribution in the medium from energy equation, besides the convective and conductive terms, the radiative term as the divergence of the radiative heat flux, i.e. $\nabla.\vec{q}_r$ also needed. This radiative term can be computed as follow [30]:

$$\nabla.\vec{q}_r = \sigma_a\left(4\pi I_b(\vec{r}) - \int_{4\pi} I(\vec{r},\vec{s})d\Omega\right) \tag{5}$$

In Eq. (5), $I(\vec{r},\vec{s})$ is the radiation intensity at the situation $\vec{r}$ and in the direction $\vec{s}$ and $I_b(\vec{r}) = \frac{\sigma(T(\vec{r}))^4}{\pi}$ is the black body radiation intensity where $\sigma_a$ is the absorption coefficient. For calculation of $\nabla.\vec{q}_r$, the radiation intensity field is essentially needed. To obtain this term, it is necessary to solve the RTE. This equation for an absorbing, emitting and scattering gray medium can be expressed as [30]:

$$(\vec{s}.\nabla)I(\vec{r},\vec{s}) = -\beta I(\vec{r},\vec{s}) + \sigma_a I_b(\vec{r}) + \frac{\sigma_s}{4\pi}\int_{4\pi} I(\vec{r},\vec{s})\phi(\vec{s},\vec{s}')d\Omega' \tag{6}$$

Where $\sigma_s$ is the scattering coefficient, $\beta = \sigma_a + \sigma_s$ the extinction coefficient and $\phi(\vec{s},\vec{s}')$ is the scattering phase function for the radiation from incoming direction $\vec{s}'$ and confined within the solid angle $d\Omega'$ to scattered direction $\vec{s}$ confined within the solid angle $d\Omega$. In this study, the phase function is equal to unity because of the assumption of isotropic scattering assumption. The boundary condition for a diffusely emitting and reflecting gray wall is:

$$I(\vec{r}_w,\vec{s}) = \varepsilon_w I_b(\vec{r}_w) + \frac{(1-\varepsilon_w)}{\pi}\int_{\vec{n}_w.\vec{s}'<0} I(\vec{r}_w,\vec{s})|\vec{n}_w.\vec{s}'|d\Omega' \quad \vec{n}_w.\vec{s}>0 \tag{7}$$

in which $\varepsilon_w$ is the wall emissivity, $I_b(\vec{r}_w)$ the black body radiation intensity at the temperature of the boundary surface and $\vec{n}_w$ is the outward unit vector normal to the surface. Since, the RTE depends on the temperature fields through the emission term $I_b(\vec{r}_w)$, thus it must be solved simultaneously with overall energy equation. RTE is an integro-differential equation that can be solved with discrete ordinates method.

In the DOM, Eq. (6) is solved for a set of n different directions, $\vec{s}_i$, i=1,2,3,…,n and integrals over solid angle are replaced by the numerical quadrature, that is:

$$\int_{4\pi} f(\vec{s})d\Omega \cong \sum_{i=1}^{n} w_i f(\vec{s}_i) \tag{8}$$

Where $w_i$ is the quadrature weight associated with the directions $\vec{s}_i$. Thus, according to this method, Eq. (6) is approximated by a set of n equations, as follows:

$$(\vec{s}_i.\nabla)I(\vec{r},\vec{s}_i) = -\beta I(\vec{r},\vec{s}_i) + \sigma_a I_b(\vec{r}) + \frac{\sigma_s}{4\pi}\sum_{j=1}^{n} I(\vec{r},\vec{s}_j)\phi(\vec{s}_j,\vec{s}_i)w_j \qquad i = 1,2,3,\ldots,n \tag{9}$$

Subjected to the boundary conditions:

$$I(\vec{r}_w,\vec{s}_i) = \varepsilon_w I_b(\vec{r}_w) + \frac{(1-\varepsilon_w)}{\pi}\sum_{\vec{n}_w.\vec{s}_j<0} I(\vec{r}_w,\vec{s}_j)|\vec{n}_w.\vec{s}_j|w_j \quad \vec{n}_w.\vec{s}_i>0 \tag{10}$$

Also $\nabla.\vec{q}_r$ is represented as:

$$\nabla.\vec{q}_r = \sigma_a\left(4\pi I_b(\vec{r}) - \sum_{i=1}^{n} I(\vec{r},\vec{s}_i)w_i\right) \tag{11}$$

At any arbitrary surface, heat flux may also be determined from the surface energy balance as:

$$\vec{q}.n(r_w) = \varepsilon_w(\pi I_b(r_w) - \sum_{\vec{n}_w.\vec{s}_j<0} I_i(r_w)|n_w.s_i|w_i) \tag{12}$$

In 2-D Cartesian coordinate system, equation (9) becomes as follows [30]:

$$\xi_i\frac{\partial I_i}{\partial x} + \eta_i\frac{\partial I_i}{\partial y} + \beta I_i = \beta S_i \qquad i = 1,2,3,\ldots,n \tag{13}$$

Where

$$S_i = (1-\omega)I_b + \frac{\omega}{4\pi}\sum_{j=1}^{n} I(\vec{r},\vec{s}_j)\phi(\vec{s}_j,\vec{s}_i)w_j \quad i = 1,2,3,\ldots,n \tag{14}$$

In fact $S_i$ is a shorthand for the radiative source function. In Eq. (14), $\omega$ is the albedo coefficient, defined as $\omega = \frac{\sigma_s}{\beta}$. The finite difference form of Eq. (13) gives the following relation for computation of the radiant intensity [30]:

$$I_{p_i} = \frac{|\xi_i|A_x I_{xi} i/\gamma_x + |\eta_i|A_y I_{yi} i/\gamma_y + \beta\forall S_{pi}}{\beta\forall + |\xi_i|A_x/\gamma_x + |\eta_i|A_y/\gamma_y} \tag{15}$$

In which $\xi_i$ and $\eta_i$ are the direction cosines for the direction $\vec{s}_i$ and $\forall$ is the element cell volume. The details of the numerical solution of RTE by DOM were also described in the previous work by the second author, in which the thermal characteristics of porous radiant burners were investigated [31].

### 3.2. Boundary Conditions

The boundary conditions are treated as no slip condition at the solid walls (zero velocity) and constant temperature of $T_w$ at all boundary surfaces. At the inlet duct section, the flow is fully developed with uniform temperature of $T_{in}$, which is assumed to be lower than $T_w$. At the outlet section, zero axial gradients for velocity components and gas temperature are employed.

For the radiative boundary conditions, the walls are assumed to emit and reflect diffusely with constant wall emissivity, $\varepsilon_w = 0.8$. The inlet and outlet sections are considered for radiative transfer as black walls at the fluid temperatures in these sections.

### 3.3. Non-Dimensional Forms of the Governing Equations

Non-dimensional forms of the governing equations consist of conservation of mass, momentum and energy can be obtained by using these dimensionless variables:

$$(X,Y)=(\frac{x}{D_h},\frac{y}{D_h}),(U,V)=(\frac{u}{U_\circ},\frac{v}{U_\circ}),P=\frac{p}{\rho U_\circ^2}$$

$$\Theta=\frac{T-T_{in}}{T_w-T_{in}},\theta_1=\frac{T_{in}}{T_w-T_{in}},\theta_2=\frac{T_w}{T_{in}},I^*=\frac{I}{\sigma T_w^4}, \quad (16)$$

$$S^*=\frac{S}{\sigma T_w^4},\tau=\beta.D_h,\ ,\ ,\ (1-\omega)=\frac{\sigma_a}{\beta},Pr=\frac{\nu}{\alpha},$$

$$Re=\frac{\rho U_0 D_h}{\mu},Pe=\mathrm{Re}.\mathrm{Pr},RC=\frac{\sigma T_w^3 D_h}{k},q_r{}^*=\frac{q_r}{\sigma T_w^4}$$

It should be mentioned that $D_h$ is the hydraulic diameter and is equal to 2h. The non-dimensional forms of the governing equations are as follows:

Conservation of mass:

$$\frac{\partial U}{\partial X}+\frac{\partial V}{\partial Y}=0 \quad (17)$$

Conservation of momentum:

$$\frac{\partial}{\partial X}\left(U^2-\frac{1}{Re}\frac{\partial U}{\partial X}\right)+\frac{\partial}{\partial Y}\left(UV-\frac{1}{Re}\frac{\partial U}{\partial Y}\right)=-\frac{\partial P}{\partial X} \quad (18)$$

$$\frac{\partial}{\partial X}\left(UV-\frac{1}{Re}\frac{\partial V}{\partial X}\right)+\frac{\partial}{\partial Y}\left(V^2-\frac{1}{Re}\frac{\partial V}{\partial Y}\right)=-\frac{\partial P}{\partial Y} \quad (19)$$

Conservation of energy:

$$\frac{\partial}{\partial X}\left(U\Theta-\frac{1}{Pe}\frac{\partial\Theta}{\partial X}\right)+\frac{\partial}{\partial Y}\left(V\Theta-\frac{1}{Pe}\frac{\partial\Theta}{\partial Y}\right)+$$

$$\frac{\tau(1-\omega)RC\theta_1\theta_2}{Pe}\left[\frac{4}{\theta_2^4}\left(\frac{\Theta}{\theta_1}+1\right)^4-\sum_{i=1}^{n}I_i^*w_i\right]=0 \quad (20)$$

Also, it should be noted that dimensionless forms of baffle height, baffle width and location of baffle from BFS are considered as below forms:

$$D=\frac{d}{D_h}\quad w_b=\frac{W_b}{D_h},\ h_b=\frac{H_b}{D_h}, \quad (21)$$

### 3.4. The Main Physical Quantities

In present work, the main physical quantities of interest in flow field and heat transfer study are the mean bulk temperature and Nusselt number. The mean bulk temperature along the channel was calculated using the following equation:

$$\Theta_b=\frac{\int_0^1\Theta U dY}{\int_0^1 U dY} \quad (22)$$

In laminar forced convection flow of a radiating gas, the energy transport from the duct wall to the gas flow depends on two related factors:

1. Fluid temperature gradient on the wall
2. Rate of radiative heat exchange on boundary surface

Therefore, total heat flux on the wall is the sum of convective and radiative heat fluxes such that $q_t=q_c+q_r=-k(\frac{\partial T}{\partial y})+q_r$. Convective, radiative and total Nusselt numbers at the walls are calculated from these heat fluxes. Convective and radiative numbers can be written by Eqs. (23) and (24), respectively.

$$Nu_c=\frac{q_c D_h}{k(T_W-T_b)}=\frac{-1}{\Theta_w-\Theta_b}\left.\frac{\partial\Theta}{\partial Y}\right|_{Y=0} \quad (23)$$

$$Nu_r=\frac{q_r D_h}{k(T_W-T_b)}=\frac{RC.\theta_1.\theta_2}{\Theta_w-\Theta_b}q_r{}^* \quad (24)$$

The function of total Nusselt number ($Nu_t=\frac{q_t D_h}{k(T_W-T_b)}$) is the sum of convective Nusselt number ($Nu_c$), and radiative Nusselt number ($Nu_r$). Accordingly, the total Nusselt number is given as follows [23], [24]:

$$Nu_t=Nu_c+Nu_r=\frac{-1}{\Theta_w-\Theta_b}\left.\frac{\partial\Theta}{\partial Y}\right|_{Y=0}+\frac{RC.\theta_1.\theta_2}{\Theta_w-\Theta_b}q_r{}^* \quad (25)$$

It should be considered that for pure convective heat transfer, total Nusselt number is equal to the convective part.

## 4 SOLUTION PROCEDURE

The fundamental governing equations are discretized using the finite volume method by integrating over an elemental cell volume. The control volumes are located utilizing the staggered grid arrangement for the x- and y- velocity components, while other variables of interest were computed at the grid nodes.

Discretized forms of the governing equations were numerically solved by making use of a line-by-line method by utilizing the Tri-Diagonal-Matrix Algorithm (TDMA). For computation of pressure correction in the iteration procedure, the SIMPLE algorithm [32] is utilized. For computation the divergence of radiative heat flux, which is needed for the numerical solution of the energy equation, the radiation intensity field is crucially needed. In the computation of radiant intensity, the numerical solution of Eq. (13), can be started with the black body assumption for the boundaries with neglecting the source term Si. In the next iteration, the general forms of Eq. (15) and its boundary condition are applied.

This procedure is repeated until the convergence criterion is met for the distribution of radiant intensity. Also, $S_6$ approximation has been used in this study (Since, in the DOM, different numbers of discrete directions can be chosen during SN approximation, the results obtained by $S_4$, $S_6$ and $S_8$ approximations were compared and there was a small difference, less 1% error, between $S_6$ and $S_8$ approximations). To simulate the incline surface of BFS and baffle in the computational domain, the blocked off method is used in this study (see Fig. 2). Based on the result of grid tests for obtaining the grid-independent solutions, an optimum grid of 560×40 is determined in the x- and y-directions, respectively. It should be mentioned that the grid is highly concentrated close to duct walls, near to the step corner and also near the baffle walls in the x- and y- directions for obtaining more accuracy in the numerical calculations. A brief overview of the solution technique can be summarized as follows:

1- A first approximation for the variables u, v, p and T at each node point is assumed.

2- From the momentum equations in the x- and y-directions, the u- and v- velocity components are calculated.

3- Pressure is calculated according to the SIMPLE algorithm.

4- The RTE is solved for computing the distribution of the radiant intensity. Then the radiative source term in the energy equation is computed at each nodal point.

5- From the energy equation, the temperature field is calculated inside the radiating medium.

6- Steps 2-5 are repeated until convergence is obtained.

About the convergency, it should be mentioned that the iterative process continues until achieving convergence of all dependent variables (velocity, pressure and temperature). For Navier-Stokes and energy equations, the convergence of solution is evaluated using a criterion taken as the values of absolute residuals in the momentum and energy equations less than $10^{-4}$, and the normalized errors in the velocity and temperature fields for each node by the following criteria:

$$Error\ \Phi = Max\left|\frac{\Phi^{n}(i,j)-\Phi^{n-1}(i,j)}{\Phi^{n}(i,j)}\right| \le 10^{-5}$$

Where $\Phi$ denotes to the velocity components, pressure and temperature and n is the iteration level. But in the numerical solution of RTE, the maximum difference between the radiative intensities computed during two consecutive iteration levels did not exceed $10^{-6}$ at each nodal point for the converged solution. By this numerical strategy, the velocity, temperature and radiation intensity distributions inside the computational domain can be obtained. It should be noted that in solving the set of governing equations with a FORTRAN computer code, and using a personal computer Intel (R) Core(TM) i5, CPU 2.53GHz and 4.00GB of RAM, the calculation time in this simulation is about 30 min.

## 5 BLOCKED-OFF METHOD

Irregular enclosures usually model using body-fitted mesh which grid lines are not necessarily orthogonal to each other. This kind of mesh demands extra complication in computations. But, in many cases, a computer program written for a regular grid can be improved to handle an irregularly shaped computational domain using the blocked-off method [21-23], [33-34]. The blocked-off method consists of drawing nominal domains around given physical domain; therefore, in this technique, the whole 2-D region is divided into two parts: active and inactive or blocked-off regions. The region where solutions are done is known as the active region and the remaining portion is known as the inactive or the blocked-off region. Therefore, by rendering some of the control volumes of the regular grid as inactive, the remaining active control volumes form the desired irregular domain with complex boundary.

By this technique, the surface of inclined backward facing step and also baffle in the present analysis are approximated by a series of fine rectangular steps (Fig. 2). It should be mentioned that the control volumes, which are inside the active region, are designated as 1 otherwise 0, as shown in Fig. 2. It is obvious that using fine grids in the interface region between active and inactive zones causes to have an approximated boundary which is more similar to the true boundary.

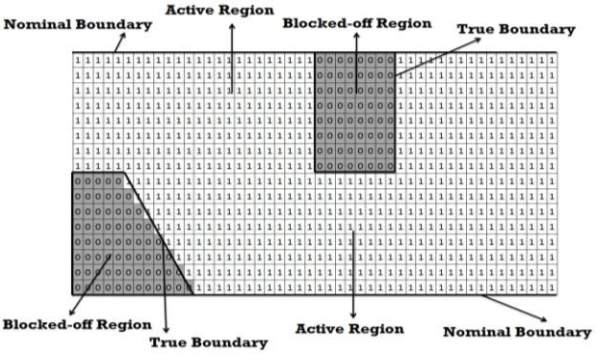


**Fig. 2** Blocked-off region in a regular grid

Idea of the blocking-off operation consists of establishing known values of the dependent variables in all inactive control volumes. If the inactive region represents a stationary solid boundary as in the case, the velocity components in that region must be equal to zero, and if the region is regarded as isothermal boundary, the known temperature must be established in the inactive control volumes. Correspondingly, when a radiant intensity enters an inactive region, its magnitude becomes zero and it takes another boundary condition if it enters again to an active region.

## 6 RESULTS AND DISCUSSION

First, it should be mentioned that validation of the numerical solution of laminar convection flow of a radiating gas along with the blocked off method were done in the previous works by the authors, in which the combined convective and radiative heat transfer problems with complex 2-D and 3-D geometries were investigated [21-22].

As it was mentioned, the numerical results of this work are presented to study the effects of baffle on separation laminar flow and combined radiation and convection heat transfer adjacent to an inclined backward facing step in a horizontal duct with expansion ratio of ER=2 and step inclination angle of $\phi = 45^{\circ}$. In numerical calculations, the Reynolds number is equal to 500, while the Prandtl number is kept constant at 0.71 to guarantee the constant fluid physical properties.

### 6.1. The effects of baffle and radiation heat transfer in forced convection flow of radiating gas

In order to show the radiation effect and also the significant effect of baffle in laminar convection flow of a radiating gas, the distribution of total Nusselt number along the bottom wall with and without considering the radiation term in energy equation and in the absence and presence of baffle are presented in Fig. 3.

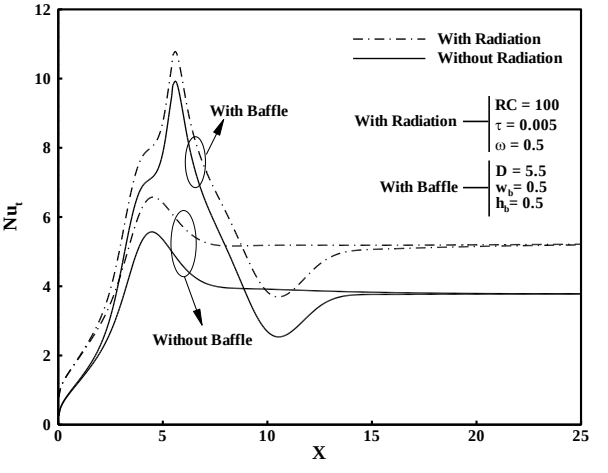


**Fig. 3** Comparison of the total Nusselt number distribution along the bottom wall in different conditions

This figure illustrates that similar pattern for total Nusselt number distribution along the bottom wall exists for both cases of radiating gas flow and non-radiating one, however, it can be seen that the radiative effect increases the value of total Nusselt number. But, according to Fig. 3, the presence of baffle causes a different trend for total Nusselt number such that the baffle effect governs the other factors in variation of Nusselt number. In the next sections, an attempt is made to study the effects of radiative parameters and also baffle geometrical factors on thermal behavior of a convection-radiation system.

### 6.2. The effects of baffle characteristics on flow and thermal behavior

Using baffles in convection-radiation systems is one of the effective methods in controlling the rate of heat transfer. In this section, the effects of height, width and location of the baffle on thermal and hydrodynamic behavior of convection flow are carried out.

#### 6.2.1. The effects of baffle location

In order to obtain the flow pattern and better explanation of results, the streamlines are plotted in

Fig. 4 at six different baffle locations in a broad range from 1.5H to 12.5H and also for the case without baffle. The effects of sudden expansion and baffle location along the duct on the flow are clearly seen from the curvatures of streamlines and separated regions.

Figure 4(g) shows that in the absence of baffle, two main recirculation zones are encountered in the flow domain at Re = 500. The primary recirculation region occurs downstream the backward step adjacent the bottom wall, whereas the secondary recirculation zone exists along the top wall. It should be noted that for small values of the Reynolds number (say for Re<350 for the test case), the secondary recirculation zone disappears. To see the effects of baffle and its location on the fluid flow behavior, Figs. 4(a) to 4(f) show the streamline contours for D=1.5, 3.5, 5.5, 7.5, 9.5 and 12.5, respectively. Comparing the streamlines in Fig. 4(g) with those plotted in Figs. 4(a) to 4(f), it is observed that the flow field has different patterns in the absence and presence of baffle, such that the baffle and its location have great effects on the flow pattern. According to Figs. 4(a) to 4(f), besides the primary and secondary recirculation zones, other three recirculation zones appear in the flow domain, such that the third and fourth recirculation zones take place adjacent to the left and right hands of baffle on the top wall, respectively, whereas the fifth recirculation zone takes place on the bottom wall downstream the baffle.

As it is seen from Fig. 4, by moving the baffle to downstream side, the length of reattachment point in the primary recirculation zone on the bottom wall increases until it reaches to reattachment point in the case without baffle. Then, by increasing the baffle location, reattachment length does not change and remains stationary. Also, it is noteworthy, while the baffle moves toward the BFS, secondary and third recirculation zones affect each other and become tied together. In addition, Fig. 4 presents that the fifth recirculation zone developed on the bottom wall as the baffle moves toward the BFS. Moreover, it should be mentioned that the effects of baffle locations on the forth recirculation zone is insignificant. To study the effect of baffle location on thermal behaviors of radiating gas flow, distributions of convective, radiative and total Nusselt numbers along the bottom wall are presented in Fig. 5. With reference to Fig. 3, it can be found that in the absence of baffle, the minimum value of total Nusselt number occurs on the bottom wall at the backward step corner, where the fluid is at rest. Also, it is seen from this figure that downstream the backward step location, the value of $Nu_t$ increases sharply in the primary recirculation region because of the flow vortices, such that the maximum local Nusselt number on the bottom wall coincides with the point of reattachment.

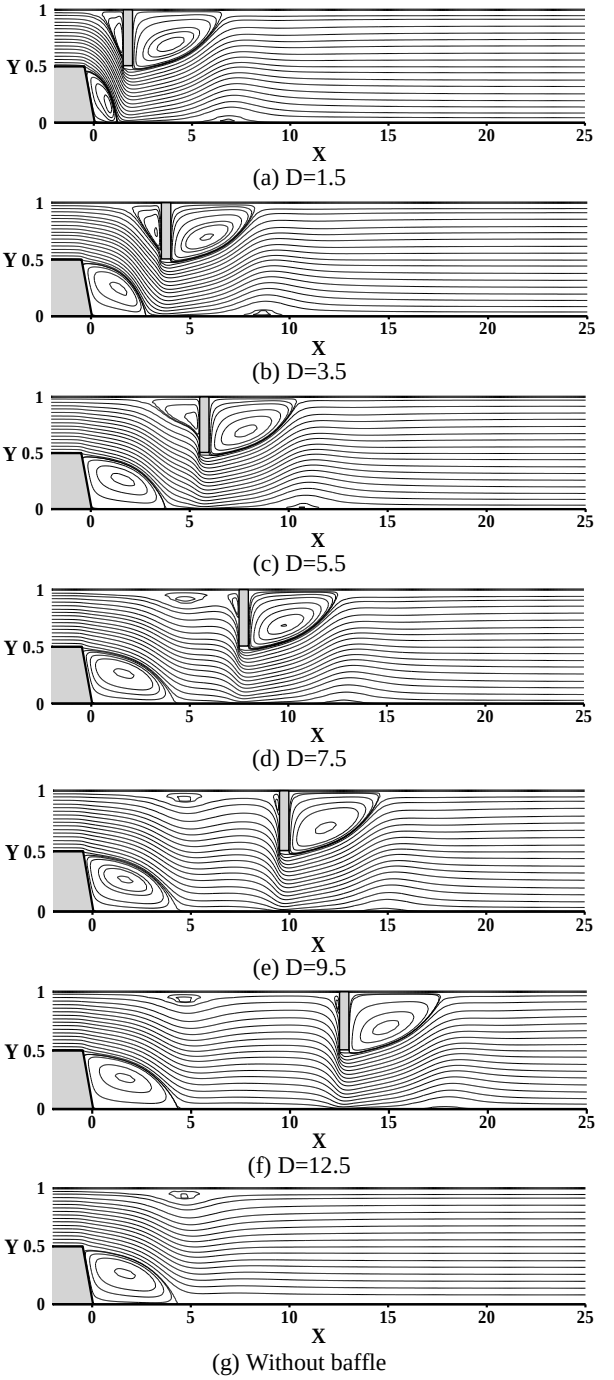


**Fig. 4** Effect of baffle location on the streamlines contours, $h_b = 0.5$ , $w_b = 0.5$

After the flow reattachment, $Nu_t$ decreases and approaches to a constant value as the distance continues to increase in the stream-wise direction. It should be noted that this constant value is due to the fully developed condition. But, as it was mentioned before,

the presence of baffle has great effect on distributions of Nusselt numbers. As it is seen from Fig. 5(c), the maximum total Nusselt number occurs on the bottom wall just below the baffle with a value which is greater than what takes place for BFS flow excluding the baffle.

This is related to the increased temperature and velocity gradients below the baffle where the flow is pushed toward the bottom wall.

Besides, it is seen from Fig. 5(c) that the maximum total Nusselt number increases as the baffle moves toward the BFS. It is important to note that in some baffle locations, total Nusselt number has a peak in reattachment point and before reaching the maximum value. Also, it should be mentioned that in the presence of baffle, $Nu_t$ has a minimum value before fully developed condition. This minimum coincides with the appearance of the fifth recirculation zone on the bottom wall, (see Figs. 4).

Figures 5(a) and 5(c) illustrate similar pattern for distribution of convective and total Nusselt number, but it can be seen that $Nu_t$ is greater than $Nu_c$ in all cases. But a different trend is seen from Fig. 5(b) for the variation of radiative Nusselt number with baffle location. This figure shows that $Nu_r$ starts from a minimum value at the backward step corner where the minimum radiative heat flux leaves the bottom wall. As the distance increases from the step corner, the amount of radiative heat flux and consequently radiative Nusselt number increases sharply and reaches to a peak, which is due to a decrease in bottom wall incident radiative heat flux incoming from the step surface. After this peak, $Nu_r$ decreases and reaches to a local minimum. Then, $Nu_r$ increases and approaches to a constant value as the distance continue to increase in the stream-wise direction.

Furthermore, Fig. 5(b) shows that the peak of the radiative Nusselt number increases by increasing the baffle location from BFS, which is due to the increase in bottom wall's outgoing radiative heat flux in radiation dominance condition.

### 6.2.2. The effects of baffle height and baffle width

To study the effects of height baffle on separation flows and distributions of Nusselt number, Figs. 6 and 7 are presented. To have better view of the flow pattern, the streamlines contours are plotted in Fig. 6 for D=3.5 and for three different baffle heights. It is observed from this figure that the baffle height has a great effect on the flow pattern and separation regions. According to Fig. 6, the effect of this parameter on fourth and fifth recirculation zones is much more, such that by a small increase in baffle height, these recirculation zones increase significantly.

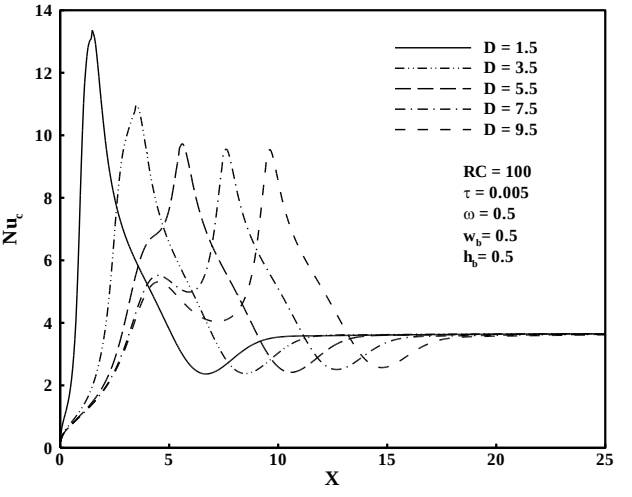


(a) Convective Nusselt number

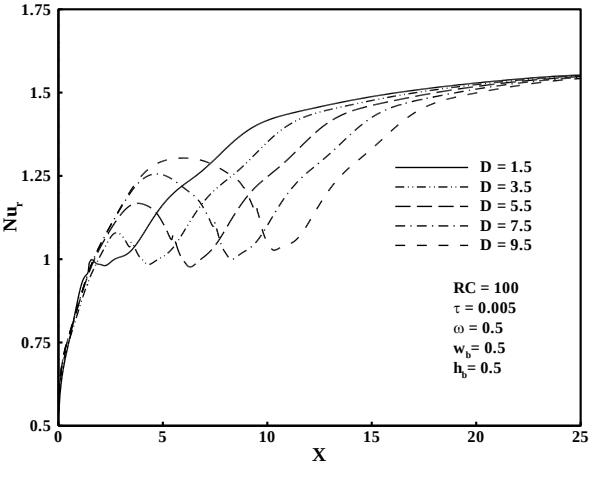


(b) Radiative Nusselt number

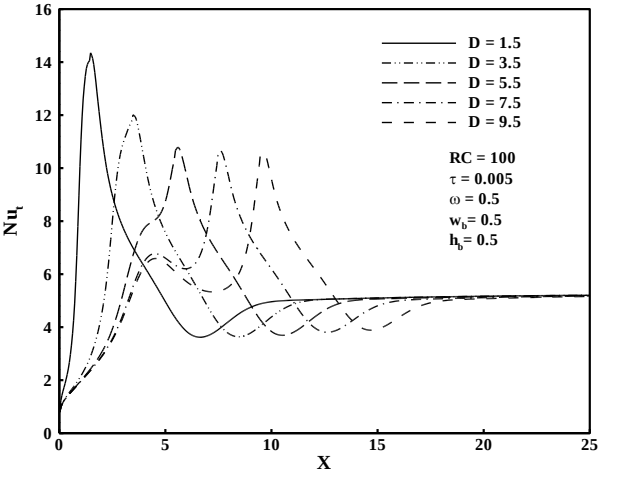


(c) Total Nusselt number

**Fig. 5** Effect of baffle location on the Nusselt number distribution along the bottom wall

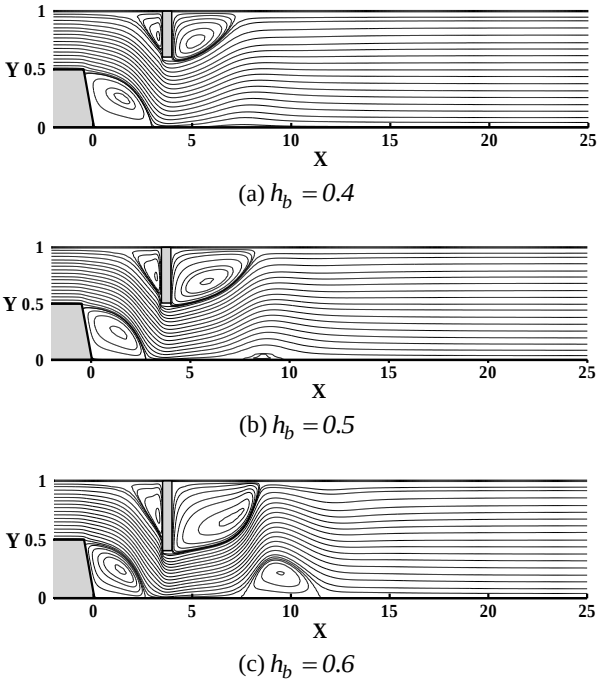


(a) $h_b = 0.4$

(b) $h_b = 0.5$

(c) $h_b = 0.6$

**Fig. 6** Effect of baffle height on the streamlines contours, D=3.5, $w_b = 0.5$

Variations of convective, radiative and total Nusselt numbers along the bottom wall for different baffle heights are plotted in Figs. 7 (a), (b) and (c), respectively. These figures clearly present that how the Nusselt number distributions are affected by this parameter. Figure 7 illustrates that the baffle height has an important role on the variations of Nusselt number distributions. This figure indicates that the values of maximum convective and total Nusselt numbers increase by increasing in the baffle height. But, this figure shows that baffle height has opposite effect on radiative Nusselt number. In other words, in the case of using baffle with small height, radiative Nusselt number is more.

Effects of baffle width on flow pattern and thermal behavior are studied in Fig. 8 and 9 by showing the streamlines contours and the total Nusselt number, respectively. If one compares the streamlines in Fig. 8 with those plotted in Fig. 6, it can be concluded that the width of baffle has a very small effect on the flow pattern in comparison to height of baffle. Also, comparison of Fig. 9 with $Nu_t$ distribution shown in Fig. 7(c) illustrates the same behavior.

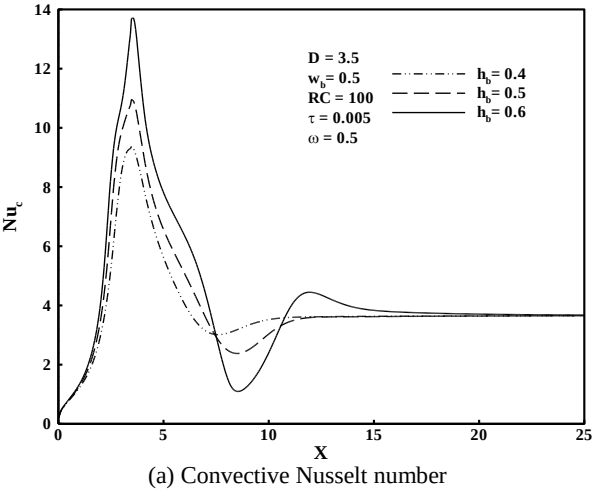


(a) Convective Nusselt number

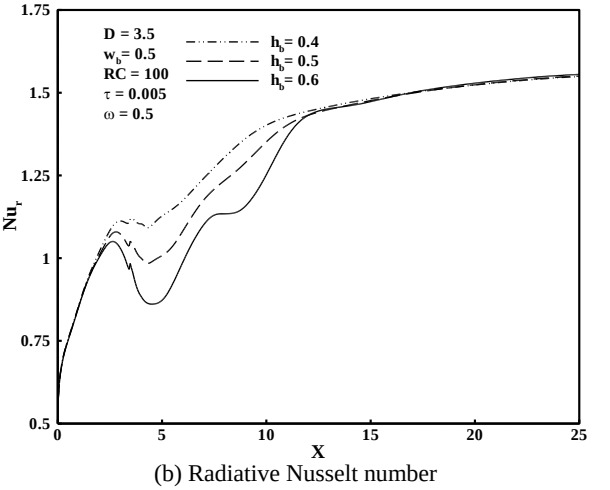


(b) Radiative Nusselt number

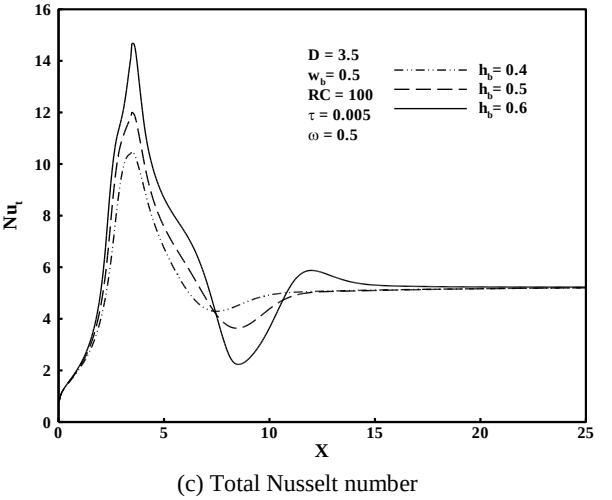


(c) Total Nusselt number

**Fig. 7** Effect of baffle height on the Nusselt number distribution along the bottom wall

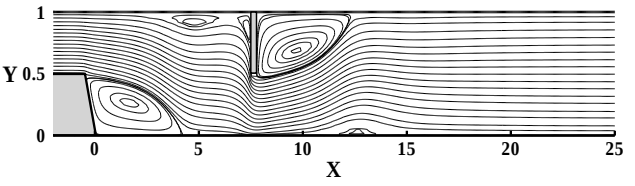


(a) $w_b = 0.3$

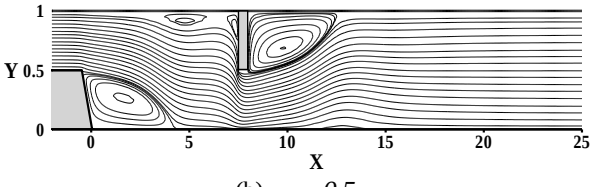


(b) $w_b = 0.5$

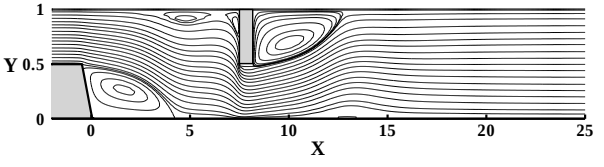


(c) $w_b = 0.7$

**Fig. 8** Effect of baffle width on the streamlines contours, D=7.5, $h_b = 0.5$

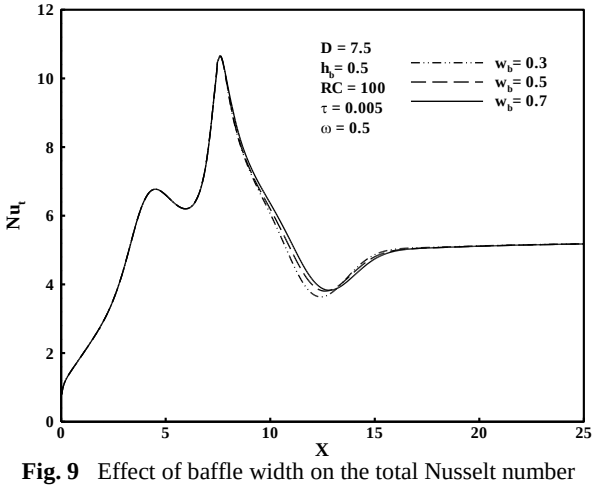


**Fig. 9** Effect of baffle width on the total Nusselt number distribution along the bottom wall

### 6.3. The effects of radiative parameters

In the convection-radiatin systems, the radiation-conduction parameter (RC), the optical thickness ( $\tau$ ) and the albedo coefficient (ω) are the main parameters that affect the thermal behaviors. In this part, the effects of these parameters are presented on thermal behaviors of the thermal systems.

#### 6.3.1. The effects of radiation–conduction parameter

In the combined radiation-conduction systems, there is a main parameter that shows the relative importance of the radiation mechanism compared with its conduction counterpart. This parameter is called Radiation-conduction parameter (RC). The distributions of convective, radiative and total Nusselt numbers along the bottom wall at different values of the RC parameter are shown in Fig. 10.

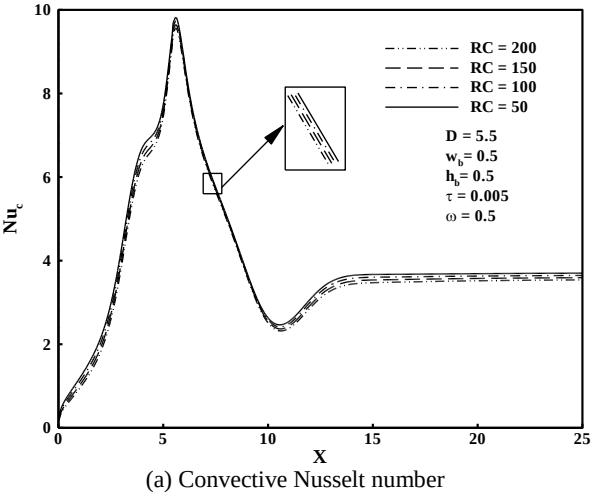


(a) Convective Nusselt number

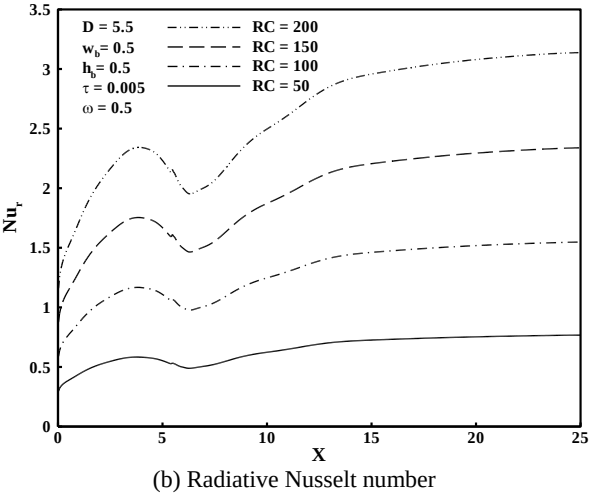


(b) Radiative Nusselt number

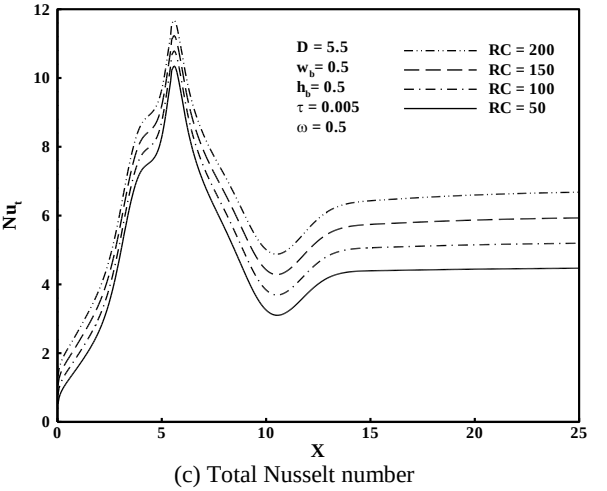


(c) Total Nusselt number

**Fig. 10** Effect of RC on the Nusselt number distribution along the bottom wall

According to Fig. 10(a), it can be concluded that the RC parameter has a small effect in convective Nusselt number, such that increasing this parameter leads to a small decrease in $Nu_c$. This is due to the fact that under the effective presence of radiation mechanism at high values of RC, the temperature field in the participating media becomes more uniform that leads to decrease in temperature gradient on the heated walls and finally decrease in convective Nusselt number. Comparison of distribution of $Nu_c$ in Fig. 10(a) with $Nu_r$ distribution shown in Fig. 10(b) illustrates that Nu distributions have different trends by variation in RC parameter, such that the radiative Nusselt number increases by increasing in RC parameter, which is due to the increase in bottom wall's outgoing radiative heat flux in radiation dominance condition. Also, it is seen from this comparison that radiation-conduction parameter has a greater influence on the radiative Nusselt number than the convective one, therefore, total Nusselt number increases by increasing in RC, as shown in Fig. 10(c).

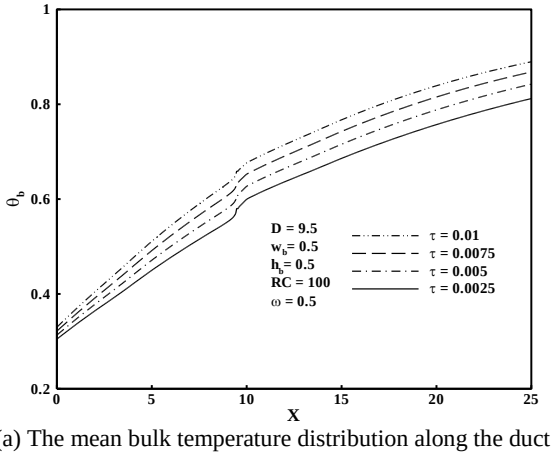


(a) The mean bulk temperature distribution along the duct

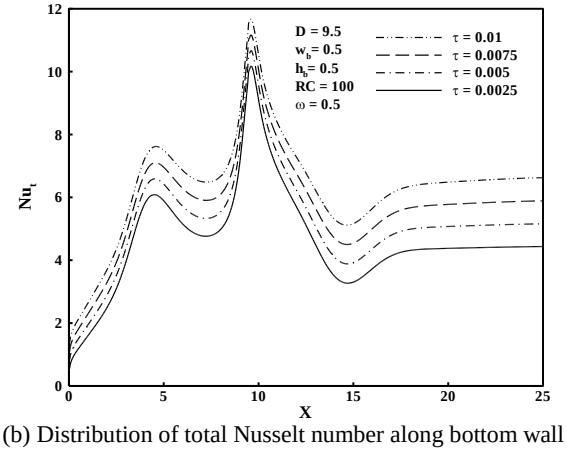


(b) Distribution of total Nusselt number along bottom wall

**Fig. 11** Effect of optical thickness on the thermal behaviors of convection-radiation systems

### 6.3.2. The effects of optical thickness

Optical thickness is an important parameter in radiating systems that affects the temperature distribution. This parameter is a well-known radiation property, such that the high values for $\tau$ means that the medium has great ability to absorb and emit radiant energy.

To study the effect of optical thickness on the thermal behavior of convection-radiation system, the mean bulk temperature distribution along the duct and also distribution of total Nusselt number on the bottom wall are plotted in Figs. 11(a) and 11(b), respectively. Figure 11(a) shows that the mean bulk temperature increases along the duct because of both convection and radiation mechanisms.

As it is seen from this figure, increase in optical thickness and consequently increase in radiation heat transfer mechanism causes an increase in the amount of the gas mean bulk temperature. It should be mentioned that the medium approaches the wall temperature at a much shorter distance from the entrance at higher optical thickness values. Also, it is seen from Fig. 11(b) that as the medium's ability to absorb and emit thermal radiation becomes greater at high values of the optical thickness; such systems have high values for the total Nusselt number.

### 6.3.3. The effects of scattering albedo

Another important parameter in participating medium is the scattering albedo that can show the ability of participating medium to scatter thermal radiation. The extreme values of scattering albedo, i.e., ω=1.0 and ω=0.0 correspond to pure scattering and non-scattering cases, respectively. Therefore, the medium changes from pure absorption to pure scattering by increasing ω from zero to unity.

The effect of scattering albedo on the total Nusselt number and mean bulk temperature is presented in Figs. 12 (a) and (b), respectively. These figures show that in the case of having participating medium with high scattering effect, the rate of heat transfer from the heated walls into convection flow decreases, such that Figs. 12(a) and (b) depict that the mean bulk temperature and total Nusselt number decrease by increasing in ω. Because, less radiative heat flux is converted to gas thermal energy in a pure scattering case compared to a pure absorption one. Besides, it can be found from Fig. 12 that when the radiation term is omitted from the energy equation in the case of no-radiation problems, the convective system has the same trend and behavior as pure scattering case with ω=1.0.

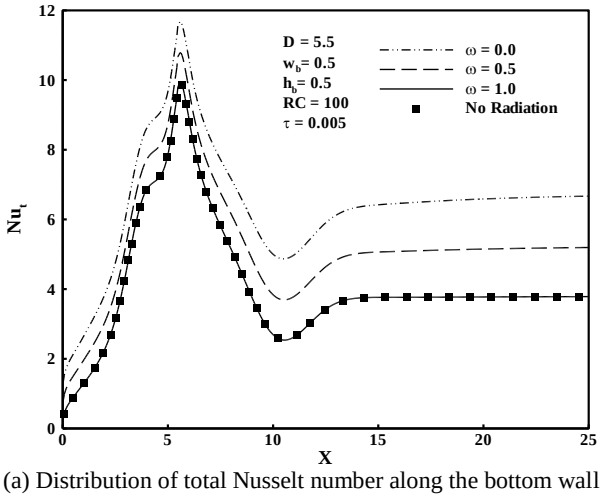


(a) Distribution of total Nusselt number along the bottom wall

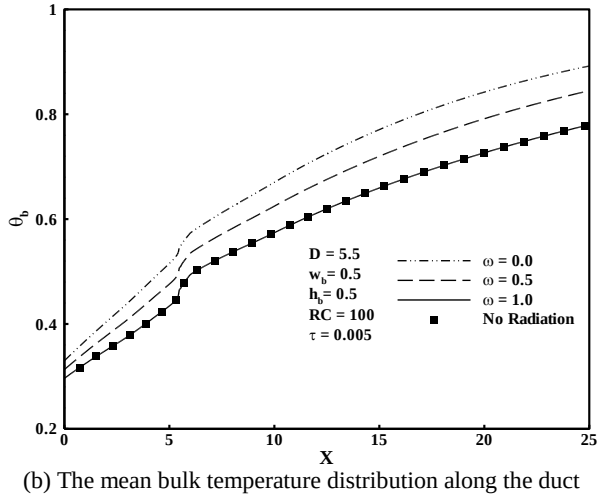


(b) The mean bulk temperature distribution along the duct

**Fig. 12** Effect of of albedo coefficient on the thermal behaviors of convection-radiation systems

## 7 CONCLUSION

The present study compared and discussed simulation of combined convection and radiation heat transfer over an inclined backward-facing step in a duct in the absence and presence of baffle. The set of governing equations including the conservations of mass, momentum and energy is solved numerically by the CFD techniques in the Cartesian coordinate system. For having more accurate and reliable results in the simulation, the gas flow is considered as a radiating medium and all of the heat transfer mechanisms including convection, conduction and radiation, are taken into account. For calculating the radiative term in the energy equation, the RTE is solved by the DOM to obtain the distribution of radiant intensity inside the radiating medium. The blocked off method is employed to simulate the incline surface of BFS and baffle. The effects of radiative parameters and characteristics of baffle (height, width and location) on the thermal behavior of the convective-radiative system are thoroughly explored by plotting the variations of streamlines contours, Nusselt number (total, radiative and convective) and mean bulk temperature under different conditions.

It was revealed that, location of baffle and baffle height have a great influence on the Nusselt number distributions, but, the effect of baffle width is very small on these parameters.

Also, it was shown that by increasing in RC the convective Nusselt number decreases along the bottom wall whereas the total Nusselt number increases. This shows that the effect of radiative Nusselt number is greater than that of convective Nusselt number on the total Nusselt number in the case of radiation dominant problem. Also, it was found that by decreasing the scattering albedo and increasing the optical thickness, the mean bulk temperature and total Nusselt number increase further.

## 8 NOMENCLATURE

| | |
|---|---|
| $A_x, A_y$ | Areas of control volume's faces normal to the x- and y- directions, respectively, ($m^2$) |
| $C_p$ | Specific heat, ($J.Kg^{-1}.K^{-1}$) |
| d | location of baffle |
| D | Dimensionless location of baffle |
| $D_h$ | Hydraulic diameter (m) |
| ER | Expansion ratio |
| $h_b$ | Baffle height |
| $H_b$ | Dimensionless baffle height |
| I | Radiation intensity, ($W.m^{-2}$) |
| $I^*$ | Dimensionless radiation intensity |
| $Nu_t$ | Total Nusselt number |
| $Nu_r$ | Radiative Nusselt number |
| $Nu_c$ | Convective Nusselt number |
| $q_t$ | Total heat flux, ($W.m^{-2}$) |
| $q_r$ | Radiative heat flux, ($W.m^{-2}$) |
| $q_c$ | Convective heat flux, ($W.m^{-2}$) |
| Pe | Peclet number |
| Pr | Prandtl number |
| Re | Reynolds number |
| RC | Radiation-conduction parameter |
| S | Radiation source function |
| $S^*$ | Dimensionless radiation source function |
| T | Temperature, (K) |
| $U_\circ$ | Average velocity of the incoming flow at the inlet section (m/s) |
| x, y | Horizontal, vertical distance, respectively, (m) |

| | |
|---|---|
| X, Y | Dimensionless horizontal and vertical coordinate, respectively |
| $x_r$ | Reattachment length (m) |
| $w_b$ | Baffle width |
| $W_b$ | Dimensionless baffle width |

**Greek Symbols**

| | |
|---|---|
| $\alpha$ | Thermal diffusivity, ($m^2.s^{-1}$) |
| $\sigma$ | Stefan Boatsman's constant = $5.67 \times 10^{-8}$, ($W.m^{-2}.k^{-4}$) |
| $\sigma_a$ | Absorbing coefficient, ($m^{-1}$) |
| $\sigma_s$ | Scattering coefficient, ($m^{-1}$) |
| $\varepsilon$ | Wall emissivity |
| $\phi$ | Step inclination angle |
| $\kappa$ | Thermal conductivity |
| $\mu$ | Dynamic viscosity $(N.s/m^2)$ |
| $\nu$ | Kinematic viscosity $(m^2/s)$ |
| $\rho$ | Density $(kg/m^3)$ |
| $\tau$ | Optical thickness |
| $\Theta$ | Dimensionless temperature |
| $\Theta_b$ | Mean bulk temperature |
| $\theta_1, \theta_2$ | Dimensionless temperature parameters |

**Subscripts**

| | |
|---|---|
| c | Convective |
| in | Inlet section |
| r | Radiative |
| t | Total |
| w | Wall |

## REFERENCES


[1] Vradis, G., Nostrand, V. L., "Laminar coupled flow downstream an asymmetric sudden expansion", Journal of Thermophysics Heat Transfer, Vol. 6, No. 2, 1992, pp. 288-295.

[2] Tylli, N., Kaiktsis L., and Ineichen, B., "Side wall effects in flow over backward-facing step: experiments and numerical solutions", Physics Fluids, Vol. 14, No. 11, 2002, pp. 3835-3845.

[3] Brakely, D., Gabriela, M., Gomes M., and Henderson, R. D., "Three - dimensional instability in flow over a backward - facing step", Journal of Fluid Mechanics, Vol. 473, 2002, pp. 167-190.

[4] Atashafrooz, M., Gandjalikhan Nassab, S. A. and Ansari, A. B., "Numerical analysis of laminar forced convection flow over backward and forward facing steps in a duct under bleeding condition", International Review of Mechanical Engineering, Vol.5, No. 3, 2011, pp. 513-518.

[5] Selimefendigil, F., Oztop, H. F., "Numerical analysis of laminar pulsating flow at a backward facing step with an upper wall mounted adiabatic thin fin", Computers & Fluids, 2013, Vol. 88, pp. 93-107.

[6] Erturk, E., "Numerical solutions of 2-D steady incompressible flow over a backward-facing step, Part I: High Reynolds number solutions", Computers & Fluids, Vol. 37, 2008, pp. 633-655.

[7] Abu-Nada, E., "Numerical prediction of entropy generation in separated flows", Entropy, 2005, Vol. 7, pp. 234-52.

[8] Abu-Nada, E., "Entropy generation due to heat and fluid flow in backward facing step flow with various expansion ratios", International Journal of Exergy, Vol. 3, 2006, pp. 419-35.

[9] Abu-Nada, E., "Investigation of entropy generation over a backward facing step under bleeding conditions", Energy Conversion and Management, Vol. 49, 2008, pp. 3237-3242.

[10] Abu-Mulaweh, H. I., "A review of research on laminar mixed convection flow over backward- and forward-facing steps", International Journal of Thermal Sciences, Vol. 42, 2003, pp. 897-909.

[11] Chen, Y. T., Nie, J. H., Hsieh, H. T., and Sun, L. J., "Three-dimensional convection flow adjacent to inclined backward-facing step", International Journal of Heat and Mass Transfer, Vol. 49, 2006, pp. 4795-4803.

[12] Atashafrooz, M., Gandjalikhan Nassab, S. A., and Ansari, A. B., "Numerical Study of Entropy Generation in Laminar Forced Convection Flow Over Inclined Backward and Forward Facing Steps in a Duct", International Review of Mechanical Engineering, Vol. 5, No. 5, 2011, pp. 898-907.

[13] Atashafrooz, M., Gandjalikhan Nassab S. A., and Ansari, A. B., "Numerical investigation of entropy generation in laminar forced convection flow over inclined backward and forward facing steps in a duct under bleeding condition", Thermal Science, Vol.18 No. 2 2014, pp. 479-492.

[14] Bahrami, A., Gandjalikhan Nassab S. A., and Hashemipour, M., "Effects of baffle on entropy generation in separated convection flow adjacent to inclined backward-facing step", Journal of Electronics Cooling and Thermal Control, Vol. 2, 2012, pp. 53-61.

[15] Nie, J. H., Chen Y. T., and Hsieh, H. T., "Effects of a baffle on separated convection flow adjacent to backward-facing step", International Journal of Thermal Sciences, Vol. 48, 2009, pp. 618-625.

[16] Oztop, H. F., Mushatet K. S., and Yilmaz, I., "Analysis of turbulent flow and heat transfer over a double forward facing step with obstacles", International Communications in Heat and Mass Transfer, Vol. 39. No. 9, 2012, pp. 1395-1403.

[17] Bouali, H., Mezrhab, A., "Combined radiative and convective heat transfer in a divided channel", International Journal of Numerical Methods for Heat & Fluid Flow, Vol. 16, 2006, pp. 84-106.

[18] Chiu, H. C., Jang, J. H., and Yan, W. M., "Mixed convection heat transfer in horizontal rectangular ducts with radiation effects", International Journal of Heat and Mass Transfer, Vol. 50, 2007, pp. 2874-2882.

[19] Chiu, H. C., Yan, W. M., "Mixed convection heat transfer in inclined rectangular ducts with radiation

effects", International Journal of Heat and Mass Transfer, Vol. 51, 2008, pp. 1085-1094.

[20] Ko M., Anand, N. K., "Three-dimensional combined convective-radiative heat transfer over a horizontal backward-facing step—A finite-volume method", Numerical Heat Transfer, Part A, Vol. 54, 2008, pp. 109-129.

[21] Atashafrooz M., Gandjalikhan Nassab, S. A., "Simulation of three-dimensional laminar forced convection flow of a radiating gas over an inclined backward-facing step in a duct under bleeding condition", Institution of Mechanical Engineers, Part C, Journal of Mechanical Engineering Science, Vol. 227. No. 2, 2012, pp. 332-345.

[22] Atashafrooz M., Gandjalikhan Nassab, S. A., "Combined heat transfer of radiation and forced convection flow of participating gases in a three-dimensional recess", Journal of Mechanical Science and Technology, Vol. 26, No. 10, 2012, pp. 3357-3368.

[23] Atashafrooz M., Gandjalikhan Nassab, S. A., "Numerical analysis of laminar forced convection recess flow with two inclined steps considering gas radiation effect", Computers & Fluids, Vol. 66, 2012, pp. 167-176.

[24] Ansari, A. B., Gandjalikhan Nassab, S. A., "Study of laminar forced convection of radiating gas over an inclined backward facing step under bleeding Condition using the blocked-off method", ASME, Journal of heat transfer, Vol. 133, 2011, Issue 7, 072702.

[25] Nouanegue, H., Muftuoglu A., and Bilgen, E., "Conjugate heat transfer by natural convection, conduction and radiation in open cavities", International Journal of Heat and Mass Transfer, Vol. 51, 2008, pp. 6054-6062.

[26] Ghaly A. Y., Elbarbary, E. M. E., "Radiation effect on MHD free convection flow of a gas at a stretching surface with a uniform free stream", Journal of Applied Mathematics, Vol. 2. No. 2, 2002, pp. 93-103.

[27] Azad, F. H., Modest, M. F., "Combined radiation and convection in absorbing emitting and anisotropically scattering gas-particulate flow", International Journal of Heat and Mass Transfer, Vol. 24, 1981, pp. 1681-1698.

[28] Yan W. M., Li, H.Y., "Radiation effects on laminar mixed convection in an inclined Square Duct", ASME Journal of Heat Transfer, Vol. 121, 1999, pp. 194-200.

[29] Yan W. M., Li, H.Y., "Radiation effects on mixed convection heat transfer in a vertical square Duct", International Journal of Heat and Mass Transfer, Vol. 44, 2001, pp. 1401-1410.

[30] Modest, M. F., "Radiative Heat Transfer", (2nd edition, McGraw-Hill, New York), 2003.

[31] Keshtkar, M. M., Gandjalikhan Nassab, S. A., "Theoretical analysis of porous radiant burners under 2-D radiation field using discrete ordinates method", Journal of Quantititative Spectroscopy & Radiative Transfer, Vol. 110, 2009, pp. 1894-1907.

[32] Patankar, S. V., Spalding, D. B., "A calculation procedure for heat, mass and momentum transfer in three-dimensional parabolic flows", International Journal of Heat and Mass Transfer, Vol. 15, No. 10, 1972, pp. 1787-1806.

[33] Patankar, S. V., "Numerical Heat Transfer and Fluid Flow", Taylor & Francis, Philadelphia, PA, Chap.7, 1981.

[34] Amiri, H., Mansouri, S. H., and Safavinejad, A., "Combined conductive and radiative heat transfer in an anisotropic scattering participating medium with irregular geometries", International Journal of Thermal Sciences, Vol. 49, 2010, pp. 492-503.